catalysts

MDPI

Article

Adsorption and Photocatalytic Reduction of Carbon Dioxide on TiO_2

Oleksandr Shtyka [1,*], Viktar Shatsila [1], Radoslaw Ciesielski [1], Adam Kedziora [1], Waldemar Maniukiewicz [1], Sergey Dubkov [2], Dmitry Gromov [2], Andrey Tarasov [2], Jacek Rogowski [1], Andrey Stadnichenko [3,4], Petr Lazarenko [2], Roman Ryazanov [5], Malgorzata I. Szynkowska-Jóźwik [1] and Tomasz Maniecki [1]

1 Institute of General and Ecological Chemistry, Faculty of Chemistry, Lodz University of Technology, 116 Zeromskiego str., 90-924 Lodz, Poland; viktar.shatsila@dokt.p.lodz.pl (V.S.); radoslaw.ciesielski@p.lodz.pl (R.C.); adam.kedziora@p.lodz.pl (A.K.); waldemar.maniukiewicz@p.lodz.pl (W.M.); jacek.rogowski@p.lodz.pl (J.R.); malgorzata.szynkowska@p.lodz.pl (M.I.S.-J.); tomasz.maniecki@p.lodz.pl (T.M.)
2 Institute of Advanced Materials and Technologies, National Research University of Electronic Technology, Shokin Square 1, Zelenograd, 124498 Moscow, Russia; sv.dubkov@gmail.com (S.D.); gromadima@gmail.com (D.G.); bloggger4@gmail.com (A.T.); aka.jum@gmail.com (P.L.)
3 Boreskov Institute of Catalysis SB RAS, 5 Ac. Lavrentiev Ave., 630090 Novosibirsk, Russia; stad@catalysis.ru
4 Faculty of Natural Sciences, Novosibirsk State University, 2 Pirogova str., 630090 Novosibirsk, Russia
5 Scientific-Manufacturing Complex "Technological Centre", 7 Shokin Square, Zelenograd, 124498 Moscow, Russia; r.m.ryazanov@gmail.com
* Correspondence: oleksandr.shtyka@p.lodz.pl

Abstract: The photocatalytic activity of TiO_2 depends on numerous factors, such as the chemical potential of electrons, charge transport properties, band-gap energy, and concentration of surface-active sites. A lot of research has been dedicated to determining the properties that have the most significant influence on the photocatalytic activity of semiconductors. Here, we demonstrated that the activity of TiO_2 in the gas-phase reduction of CO_2 is governed mainly by the desorption rate of the reaction intermediates and final products. This indicates that the specific surface area of TiO_2 and binding strength of reaction intermediates and products are the main factors affecting the photocatalytic activity of TiO_2 in the investigated process. Additionally, it was shown that rutile exhibits higher photocatalytic activity than anatase/rutile mixtures mainly due to its high efficiency in the visible portion of the electromagnetic spectrum.

Keywords: photocatalysis; CO_2 reduction; TiO_2; adsorption; deactivation; rutile; anatase

check for updates

Citation: Shtyka, O.; Shatsila, V.; Ciesielski, R.; Kedziora, A.; Maniukiewicz, W.; Dubkov, S.; Gromov, D.; Tarasov, A.; Rogowski, J.; Stadnichenko, A.; et al. Adsorption and Photocatalytic Reduction of Carbon Dioxide on TiO_2. *Catalysts* **2021**, *11*, 47. https://doi.org/10.3390/catal11010047

Received: 30 November 2020
Accepted: 29 December 2020
Published: 31 December 2020

Publisher's Note: MDPI stays neutral with regard to jurisdictional claims in published maps and institutional affiliations.

Copyright: © 2020 by the authors. Licensee MDPI, Basel, Switzerland. This article is an open access article distributed under the terms and conditions of the Creative Commons Attribution (CC BY) license (https://creativecommons.org/licenses/by/4.0/).

1. Introduction

Photocatalytic reactions, such as water splitting [1,2], oxidation of volatile organic compounds [3,4], organic synthesis [5,6], and reductive fixation of carbon dioxide [7,8], are of great importance from both fundamental and practical points of view. The typical heterogeneous photocatalysts used in these processes are metal-free organic compounds [9,10] and semiconductor materials [11]. Upon the ultraviolet and visual light (UV–VIS irradiation, these materials can generate electron-hole pairs which then are separated and transferred to the surface where they participate in redox reactions (if not recombined) [12]. Among various materials that have been studied for photocatalysis, titania (TiO_2) is of great interest due to its high photocatalytic activity, high physical and chemical stability, nontoxicity, and low-cost [13–15]. However, there are two major challenges facing titania photocatalysts for common applications: (i) a large band gap (3.3 eV) which limits its photoabsorption to the ultraviolet (UV) light only, and (ii) fast recombination of electron-hole pairs that limits the photocatalytic efficiency (typical for all semiconductors) [16,17].

Therefore, a great deal of research has been dedicated to improving the performance of titania, such as surface modification [18], doping [19], coupling with other materials [20],

as well as optimization of physicochemical properties via varying preparation [21] and treatment conditions [22]. Various factors that affect the photocatalytic activity have been reported, including crystal structure (anatase or rutile), particle size, surface area, and the presence of surface hydroxyls [23–25]. These properties can be easily altered via heat treatment of the TiO_2 in various gas atmospheres. For instance, high-temperature treatment in air was reported to intensify phase transformation from anatase to rutile and to decrease specific surface area and concentration of surface hydroxyls [26–28].

In most of the studies, the attempt is made to correlate the photocatalytic activity with only one or a few physical properties of the photocatalyst. Generally, it can be concluded that the most prominent effect on the photocatalytic activity provides the coexistence of several titania polymorphs. This effect is usually assigned to a lower energy gap of the mixed phase TiO_2 than that of pure phases [29]. However, it is also worth mentioning that despite the lower band gap of pure rutile, anatase exhibits better photocatalytic properties [30]. This effect indicates that other properties, apart from the band gap, also effect the photocatalytic performance. Particularly, it was hypothesized that the good photocatalytic activity of mixed-phase TiO_2 is due to the transfer of photo-generated electrons from anatase to a lower energy rutile electron-trapping site. This electron transfer reduces the recombination rate of anatase by increasing the separation between the electron and hole, resulting in greater photocatalytic reactivity [31–33]. More interestingly, T. Bak et al. investigated the effect of several defect-related properties, including the concentration of surface-active sites, the Fermi level, the charge transport, and the band gap of pure TiO_2 on its photocatalytic performance in the oxidation of methylene blue [34]. The obtained results indicated that the photocatalytic activity of TiO_2 was influenced significantly by the concentration of surface-active sites and Fermi level while the band gap and charge transport had a minor impact [34]. The effect of specific surface on the photocatalytic properties of TiO_2 is also not as straightforward as it may seem. It can be hypothesized that the high specific area is beneficial as it improves the adsorption of the target molecules onto the surface of titania [25,35].

However, recently, we have shown that during the photocatalytic reduction of carbon dioxide, the TiO_2 deactivates reversibly due to the slow desorption and consequent accumulation of reaction products on its surface [36]. This indicates that the high specific surface area of TiO_2 may, on the contrary, be a negative factor affecting its photocatalytic activity. Therefore, great care is needed in drawing conclusions on the decisive factors of activity in photocatalytic reactions and in rationalizing the correlations between photocatalytic properties of a semiconductor and its physicochemical properties.

The work is aimed to evaluate separately the influence of each physicochemical property of TiO_2 on its photocatalytic performance in the gas-phase CO_2 reduction. The properties of titania, such as phase composition, specific surface area, and band gap energy, were tuned by adjusting calcination temperature. Special attention was given to the initial adsorption of carbon dioxide on the surface of titania and subsequent desorption of photocatalytic products.

2. Results and Discussion

2.1. Physicochemical Properties of Pristine and Calcinated TiO_2 Samples

The results of physicochemical characterization of TiO_2 samples are summarized in Table 1. According to the obtained results, the raw TiO_2 had a specific surface area (SSA BET) of about 57 m^2. It contained mainly anatase phase (88%) with crystallite size of 18 nm and possessed a band gap of 3.291 eV, which is close to that reported elsewhere [37,38].

Table 1. Physicochemical properties of TiO_2 samples.

Sample	BET SSA, m^2/g	Phase Composition				Band Gap, eV
		Anatase,%	Average Crystallite Size, nm	Rutile,%	Average Crystallite Size, nm	
TiO_2-pristine	57	87.8	18	12.2	25	3.291
TiO_2-C500	56	84.3	19	15.7	30	3.389
TiO_2-C700	16	-	-	100.0	85	3.071
TiO_2-C1000	4	-	-	100.0	156	3.036

The increase in calcination temperature up to 500 °C did not significantly alter the properties of TiO_2; only a slight increase in the size of titanium dioxide crystallites was observed along with the broadening of band gap up to 3.389 eV. Similar results were reported by H. Lin et al. [39] and K. Vajda et al. [40]. They observed the increase in band gap of TiO_2 with an increase in its particle size (for crystallites with a size of above 15 nm). Such a result was attributed to a higher amount of bulk defects which induce delocalization of molecule orbitals and create shallow/deep traps in the semiconductor [39]. A further increase in calcination temperature up to 700 °C resulted in complete phase transformation from metastable anatase to stable rutile and a decrease of the band gap energy value. The process was accompanied by an increase in the size of the crystallites (due to agglomeration) and a significant decrease in BET surface area down to 16 m^2/g (Figure 1, Table 1). With a further increase in temperature to 1000 °C, the size of titanium dioxide particles increased from 85 to 156 nm while the SSA reduced to 4 m^2/g.

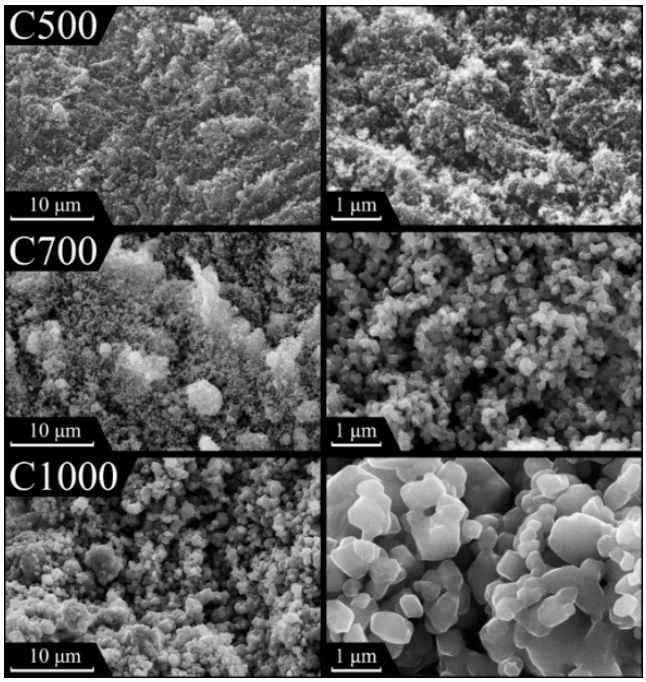


Figure 1. The SEM images of TiO_2 samples calcinated at different temperatures.

The results of XPS measurements revealed that irrespective of calcination temperature, the Ti remained mainly in its tetravalent state. The increase in calcination temperature above 500 °C led to a prominent increase in hydroxyl groups on the surface of TiO_2 and to a decrease in oxygen content in titanium oxide lattice as evidenced by the decrease in O-Ti/Ti ratio (Table 2). It can be hypothesized that the oxygen vacancy sites were formed upon calcination at high temperatures and acted as adsorption sites for water vapor presented in air, leading to the formation of hydroxyls [41,42].

Table 2. Surface elemental composition of TiO_2 samples.

Sample	Total Ti2p Species	O1s (eV)			O-Ti/Ti Ratio
		O-Ti (529.9)	Ti-OH (531.5)	Total	
TiO_2-pristine	29.28	63.09	7.64	70.73	2.15
TiO_2-C500	30.37	64.82	4.81	69.63	2.13
TiO_2-C700	31.03	57.83	11.13	68.96	1.86
TiO_2-C1000	29.89	57.26	12.85	70.11	1.92

The results of XPS measurements are in good agreement with outcomes from TOF-SIMS analysis. As can be seen in Figure 2, the emission of secondary TiO_3H^- ions increased steadily with increase in the calcination temperature. Apart from it, the significant intensification of emission of TiO^- and related ions was observed at 700 °C, which can be due to change of orientation of surface crystallites as a result of anatase-to-rutile phase transition. At 1000 °C, the intensity of these ions decreased due to substantial contraction of specific surface area of the calcinated sample.

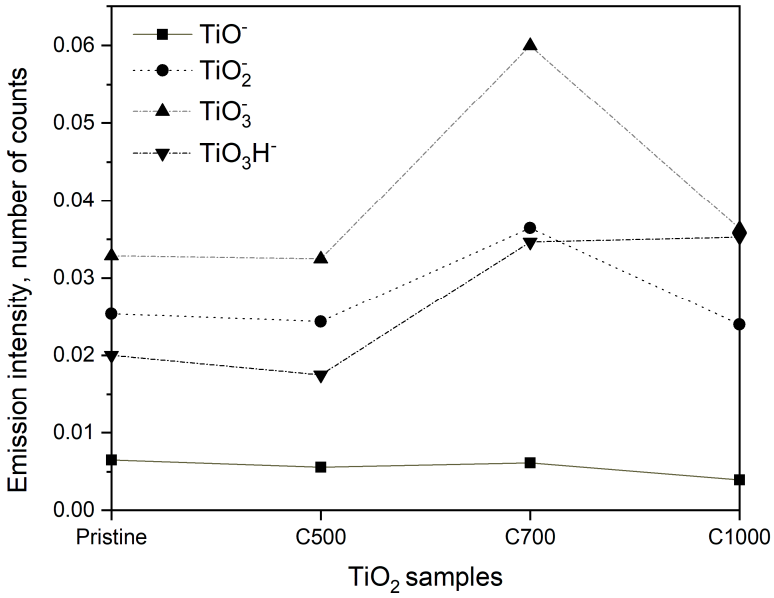


Figure 2. Emission of negative secondary ions from the cleaned surface of TiO_2 samples.

As was expected, the titanium oxide intrinsically exhibited strong absorption of electromagnetic radiation in the UV region (Figure 3). With an increase in calcination temperature, the ability of TiO_2 to adsorb UV light significantly deteriorated. Importantly, it can be seen in the TiO_2-C1000 sample that the UV reflectivity increased twofold in comparison to that of pristine titanium dioxide. Such effect is related to the superficial morphology of TiO_2 particles. As discussed previously, at high temperatures, TiO_2 particles adhere together to form large agglomerates (Table 1). These agglomerates have a smoother surface than small particles resulting in higher reflection of incident photons [43,44]. The calcination treatment did not significantly alter the adsorption of electromagnetic radiation in the entire visible spectrum, i.e., only a slight red-shift was observed in the optical spectra of TiO_2 calcinated at 700 and 1000 °C, which was related to the anatase-to-rutile phase transition.

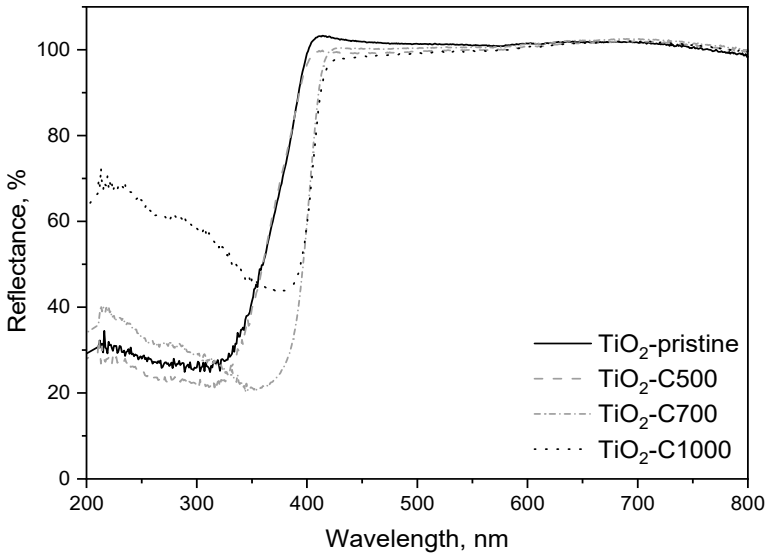


Figure 3. Reflectance spectra of TiO_2 samples calcinated at different temperatures.

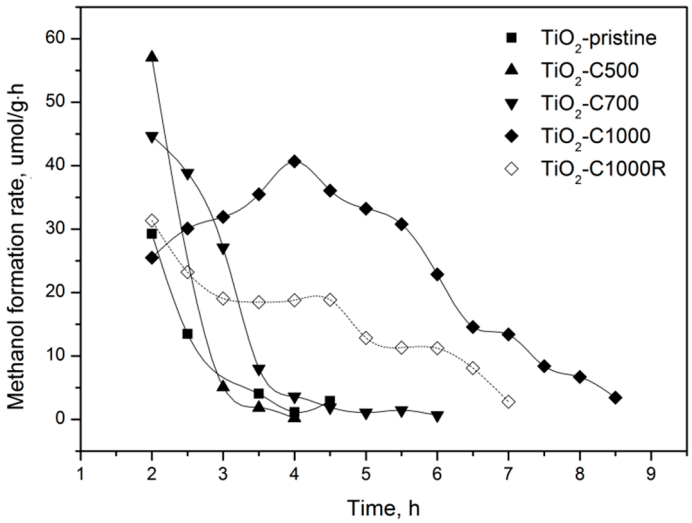


Figure 4. The photocatalytic activity of TiO_2 samples under UV–VIS irradiation as a function of reaction time on stream at 30 °C.

2.2. Photocatalytic and Adsorption Properties of TiO_2 Samples

The results of the photocatalytic measurements showed that the investigated samples at ambient temperature easily underwent deactivation, as can be seen by the sharp decrease of methanol formation rate with time on stream (Figure 4). The only exception was the TiO_2-C1000 sample which demonstrated relatively stable photocatalytic activity over the 5 h. As was discussed previously, the deactivation of the photocatalysts in this process can be due to the accumulation of reaction products on the surface of the photocatalyst hindering the adsorption of reagents [36]. The IR measurements indeed showed that the formed methoxy groups (2819, 2897, and 2922 cm^{-1}) hardly desorbed from the surface of photocatalysts irrespective of their specific surface area (Figure 5B). For example, according to the FTIR measurements, approximately only 35% of total adsorbed methanol desorbs from the surface of pristine TiO_2 when purged with inert gas for 1 h under UV–VIS irradiation (Figure 6). In the case of TiO_2-C700, about 45% of organic groups were removed under the same conditions, while in the case of TiO_2-C1000 it was above 65%. Nevertheless, it is worth mentioning that the observed deactivation of photocatalysts is reversible as they can be partially regenerated by heating at 300 °C in the flow of reaction mixture.

For instance, the TiO_2-C1000 regenerated for one hour (TiO_2-C1000R) exhibited lower but comparable photoactivity as that observed at the beginning of the photocatalytic process.

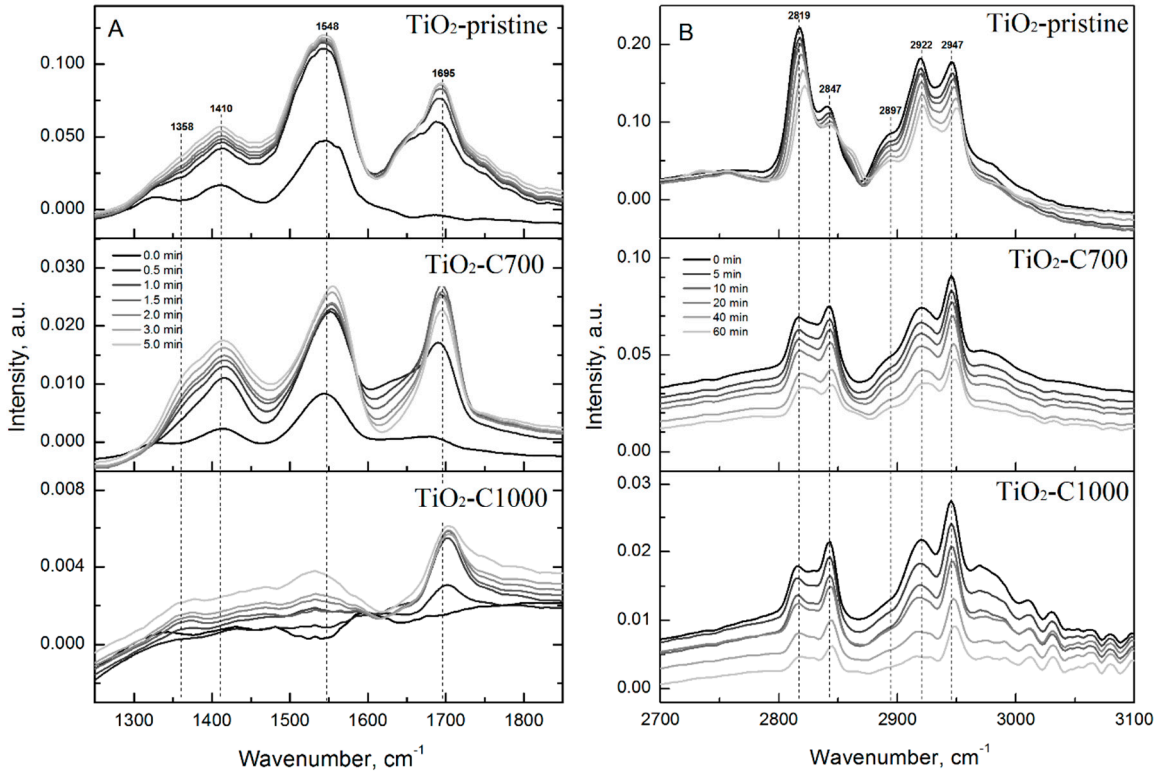


Figure 5. Adsorption of CO_2 (**A**) and desorption of methanol (**B**) on/from the surface of TiO_2 samples.

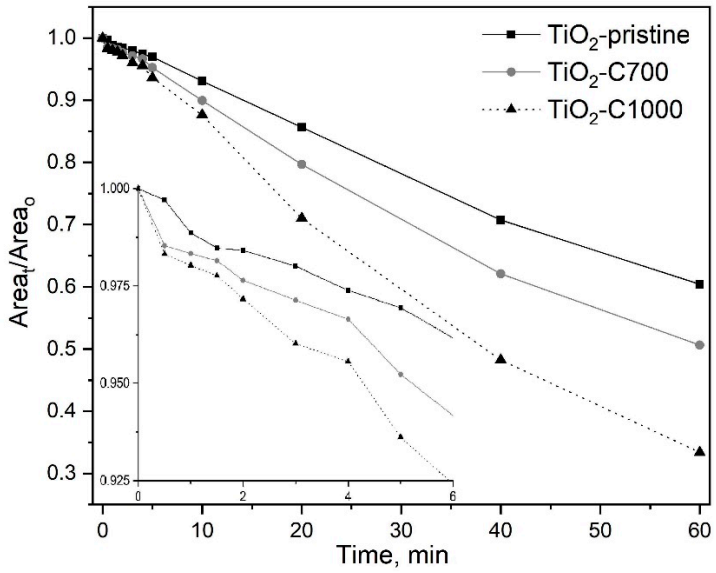


Figure 6. Desorption rate of organic groups from the surface of TiO_2 samples under UV–VIS irradiation at room temperature.

Although the accumulation of reaction products on the surface of TiO_2 samples did influence the photocatalytic process, this effect alone cannot explain the differences in photocatalytic activity of TiO_2 samples as the differences in desorption rates among them were rather small (Figure 6).

The FTIR studies on the adsorption of CO_2 on the surface of titania revealed also that TiO_2-C1000 was characterized by not only a lower amount of CO_2 adsorbed but also by a slower adsorption rate than that of the pristine sample. As can be seen from Figure 5A, the adsorption of CO_2 proceeds readily, as evidenced by the notable increase in intensities of characteristic peaks for carbonate species (1358–1695 cm^{-1}) immediately after the beginning of the process. On the other hand, the adsorption on the surface of TiO_2-C1000 started only after half of a minute, as is evident from the appearance of weak IR bands. Thus, it can be hypothesized that at room temperature the activity of TiO_2 in photocatalytic reduction of CO_2 is governed by adsorption-desorption factors but not by photocatalytic ones. More particularly, we believe that the lower CO_2 adsorption rate along with the slightly higher desorption rate of organic groups (Figure 6) is the reason for the higher stability (but not activity) of TiO_2-C1000 in the photocatalytic reduction of CO_2 process when conducted at room temperature.

Therefore, to reveal the photocatalytic properties of investigated samples, the photocatalytic process was conducted at 100 °C. At this temperature, the desorption of both reaction intermediates and products can be partially assured. As can be seen from the obtained results (Figure 7) all samples exhibited no significant loss in photocatalytic activity with time on stream indicating a sufficient level of desorption of reaction products from the surface of the photocatalyst. It is worth mentioning that the thermal effect alone has a small effect on the rate of methanol formation rate (about 12–15% of total photocatalytic activity) and in all calculations was accounted for. When it is applied simultaneously with electromagnetic radiation, the synergetic effect on the photocatalytic process was observed, as evidenced by the prominent increase in the rate of methanol formation (in comparison to that observed at room temperature, Figure 4). Such effect was due to a higher number of electrons having enough energy to overcome the band gap and reach the conduction gap.

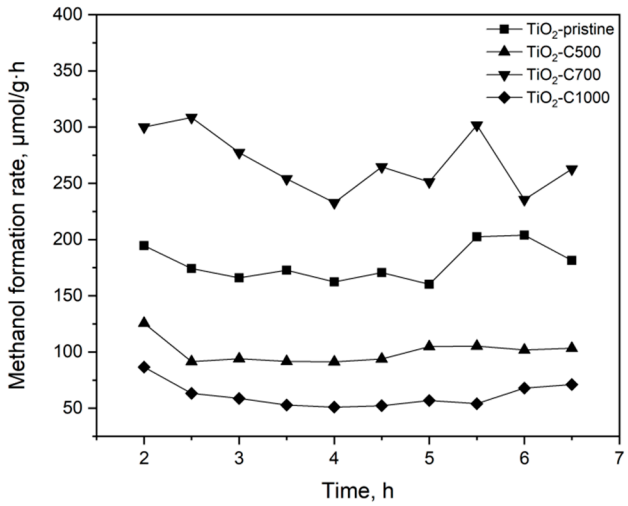


Figure 7. The photocatalytic activity of TiO_2 samples under UV–VIS irradiation as a function of reaction time on stream at 100 °C.

It is generally accepted that the photocatalytic activity of anatase is superior to that of rutile. The lower activity of rutile is usually explained in terms of bulk charge carrier transport properties [30] as well as adsorption properties [45]. The photocatalytic measurements, however, showed that a TiO_2-C700 (i.e., rutile) exhibited significantly higher activity than the pristine sample containing 88% anatase (Figure 7).

The higher activity of rutile in this process was primarily due to high efficiency in the visible portion of the electromagnetic spectrum. The experiments performed with the use of cutoff filters demonstrated that both TiO_2-pristine and TiO_2-C700 had comparable photocatalytic activities in the UV spectrum which were in the range of 50–65 μmol/g·h (Figure 8). Under visible light irradiation, on the other hand, the TiO_2-C700 was the only photocatalyst

demonstrating significant levels of activity, about 20–30 μmol/g·h. The secondary factors which probably contributed to the higher photocatalytic activity of TiO_2-C700 are lower specific surface area (better desorption of reaction products) and higher concentration of surface hydroxyl groups which inhibit the electron-hole recombination [46]. The low number of OH functional groups can be also the reason for the low activity of TiO_2-C500, which otherwise has properties similar to the pristine sample (Figure 7). The least active sample among the photocatalysts was TiO_2-C1000, which was characterized by the biggest particle size and consequently the lowest specific surface area. As discussed previously, this negatively influences the adsorption of both reagents and electromagnetic irradiation.

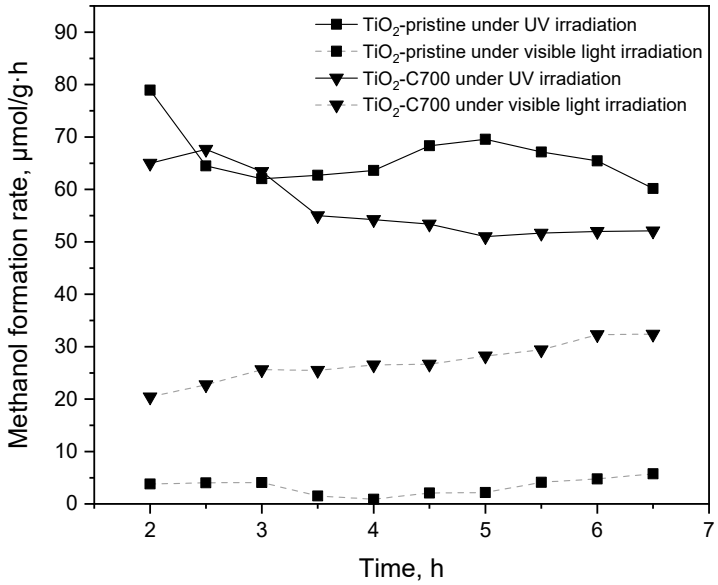


Figure 8. The photocatalytic activity of TiO_2 samples under UV and visible light irradiation as a function of reaction time on stream at 100 °C.

3. Experimental Part

3.1. Modification of TiO_2

The TiO_2 powder (P-25) was obtained from a commercial supplier (Chempur, Poland). To modify the physicochemical properties of TiO_2, it was placed in an oven and calcinated at temperatures ranging from 500 °C to 1000 °C for 4 h. Next, the calcinated TiO_2 samples were ultrasonically dispersed in distilled water for 30–45 min. The obtained suspension was carefully filtered in a way that achieved uniform deposition of TiO_2 layer on the surface of the woven filter. The obtained TiO_2/woven filter samples were then placed in the oven and dried overnight at 100 °C. The resultant sample was denoted as TiO_2-C(x), where x (500, 700, or 1000) represents the calcination temperature.

3.2. Physicochemical Characterization

The specific surface area of raw and calcinated TiO_2 was estimated from nitrogen adsorption/desorption measurements at −196 °C using a Sorptomatic 1900 instrument (Carlo Erba, Milan, Italy). Before measurements, powder samples were outgassed under vacuum at 300 °C.

The phase composition of photocatalysts was studied with a PANalytical X'Pert Pro MPD diffractometer (Malvern Panalytical Ltd., Malvern, UK) using a CuKα radiation source (λ = 1.5418 Å) in 2θ range of 5–90°. The average size of TiO_2 crystallites was calculated using the Scherrer equation while the weight fraction of TiO_2 polymorphs was estimated using reference intensity ratio (RIR) method.

The secondary ions mass spectra were recorded with a TOF-SIMS IV mass spectrometer (IONTOF, Münster, Germany) equipped with a Bi liquid metal ion gun and a high

mass resolution time of flight mass analyser. For each sample, three surface spectra were taken from approximately 100 × 100 μm area. The number of recorded counts of selected ions was normalized based on the value of total counts. Prior to measurement, powder specimens were pressed into pellets.

The XPS spectra were measured using a VG ESCALAB HP photoelectron spectrometer (Thermo Electron North America LLC, Waltham, MA, USA) with a non-monochromated primary radiation source (MgKα line of hν = 1253.6 eV) with a power 150 W. Sample powders were pressed into pills (7 × 15 mm, 2 mm). Before the experiments, the spectrometer binding energy (BE) scale was calibrated based on the energy position of metallic gold Au4f7/2 (84.0 eV) and copper Cu2p3/2 (932.7 eV) lines. A titanium Ti2p3/2 line with a maximum at a binding energy 458.6 eV was used as an internal standard [47]. To analyze the quantitative composition of the samples and the chemical state of the elements on the surface, the core-level spectra of the elements (Ti2p, C1, O1s) were recorded. The measurement accuracy of XPS binding energy was 0.1 eV. The spectra were fitted with the individual components using the Gauss and Lorentz functions after Shirley background subtraction. The spectra were processed using XPS-Calc software (Thermo Electron North America LLC, Waltham, MA, USA) tested previously on model catalytic systems [48] and dispersed powder catalysts [49].

The diffuse reflectance spectra of the powder samples were measured using Cary 5000 UV–VIS–NIR spectrophotometer with an integrating sphere (Agilent, Santa Clara, CA, USA) in the 200–800 nm wavelength range. Reflectance spectra were recorded with a spectral resolution of 1 nm.

The adsorption-desorption measurements were performed using IR Tracer-100 FTIR spectrometer (Shimadzu, Kyoto, Japan) equipped with an MCT detector. During the experiments, the 5% CO_2-95% Ar and 5% CH_3OH-95% Ar mixtures were used. The gas flow rate was 10 mL/min. The desorption rate of adsorbed methanol was calculated as a change or area of corresponding IR peaks during the purging with an inert gas under UV-VIS irradiation. All measurements were performed at 30 °C.

The surface morphology of the investigated samples was studied by HITACHI scanning electron microscope (Hitachi High-Tech, Tokyo, Japan), equipped with EDS energy dispersive spectrometer (Thermo Noran, Worona Road Madison, WI, USA).

3.3. Photocatalytic Activity Measurement

A detailed description of a photocatalytic reactor has been given elsewhere [36]. Briefly, the photocatalytic reduction of CO_2 was performed in a flow reactor equipped with a cooling jacket, a heater, and a quartz window. Two paired, high-pressure mercury lamps (POLAMP LRF 400W) were used as a source of UV-VIS light. The area of TiO_2 surface exposed to UV-vis irradiation was 10.18 cm^2. For performing the photocatalytic tests under either UV or visible light irradiation alone, special cutoff filters were applied. The surface area exposed to the irradiation, in this case, was equal to 2.01 cm^2. The process conditions were as follows: the temperature of the semiconductors—30 and 100 °C; the reaction mixture—5% vol. H_2O/95% vol. CO_2; and total gas flow—0.8 mL/min. The first measurements were taken after at least 2 h on stream. The analysis of reaction products was carried out by an on-line gas chromatograph equipped with a flame ionization detector and a capillary HP PLOT/Q column. The yield of an organic compound was calculated according to the following equation:

$$Y_{compound}\ (\mu mol/g{\cdot}h) = \text{Molar flow rate}_{\ compound} \ / \ g_{catalyst} \times 60 \quad (1)$$

4. Conclusions

The physical properties of titanium oxide, such as the surface morphology and composition and the adsorption of electromagnetic radiation and reaction reagents, can be controlled to some extent by varying the temperature of the calcination process. The increase in calcination temperature resulted in an increase in particle size (decrease of specific

surface area), a higher concentration of surface hydroxyls, and a lower band-gap energy (at 700 °C due to anatase–rutile phase transformation). The activity of TiO_2 samples in the process of photocatalytic reduction of CO_2 at room temperature was found to be dependent primarily on the rate of desorption of reaction products from the surface of TiO_2. The samples with a high specific surface area (above 16 m^2/g) easily underwent deactivation with time on stream due to the accumulation of reaction products, while the sample with a low specific area (4 m^2/g) demonstrated relatively stable photocatalytic activity over the 5 h. On the other hand, when the process was performed at 100 °C (the adsorption factor is partially suppressed) the low specific surface was found to be negatively impacting the photocatalytic activity of the investigated samples. The most important factor, under such conditions, was improved utilization of visible light irradiation. This was the main reason for the enhanced photocatalytic activity of rutile in comparison to that of anatase/rutile mixture. To summarize, one of the most essential factors that should be considered while developing highly active photocatalysts for gas-phase reduction of carbon dioxide is finding the optimal trade-off between its adsorption and desorption properties.

Author Contributions: Conceptualization, D.G. and M.I.S.-J.; investigation, O.S., V.S., R.C., A.K., W.M., A.T., J.R., A.S., P.L., and R.R.; methodology, S.D.; supervision, T.M.; writing—original draft, O.S.; writing—review and editing, T.M. All authors have read and agreed to the published version of the manuscript.

Funding: This research was funded by the Russian Science Foundation (Project No. 19-19-00595).

Institutional Review Board Statement: Not applicable.

Informed Consent Statement: Not applicable.

Data Availability Statement: Not applicable.

Conflicts of Interest: The authors declare no conflict of interest.

References

1. Hisatomi, T.; Kubota, J.; Domen, K. Recent advances in semiconductors for photocatalytic and photoelectrochemical water splitting. *Chem. Soc. Rev.* **2014**, *43*, 7520–7535. [CrossRef] [PubMed]
2. Kudo, A.; Miseki, Y. Heterogeneous photocatalyst materials for water splitting. *Chem. Soc. Rev.* **2009**, *38*, 253–278. [CrossRef]
3. Shah, K.W.; Li, W. A review on catalytic nanomaterials for volatile organic compounds VOC removal and their applications for healthy buildings. *Nanomaterials* **2019**, *9*, 910. [CrossRef] [PubMed]
4. Huang, Y.; Ho, S.S.H.; Lu, Y.; Niu, R.; Xu, L.; Cao, J.; Lee, S.C. Removal of indoor volatile organic compounds via photocatalytic oxidation: A short review and prospect. *Molecules* **2016**, *21*, 56. [CrossRef] [PubMed]
5. Friedmann, D.; Hakki, A.; Kim, H.; Choi, W.; Bahnemann, D.W. Heterogeneous photocatalytic organic synthesis: State-of-the-art and future perspectives. *Green Chem.* **2016**, *18*, 5391–5411. [CrossRef]
6. Michelin, C.; Hoffmann, N. Photocatalysis applied to organic synthesis—A green chemistry approach. *Curr. Opin. Green Sustain. Chem.* **2018**, *10*, 40–45. [CrossRef]
7. Albero, J.; Peng, Y.; García, H. Photocatalytic CO_2 Reduction to C^{2+} Products. *ACS Catal.* **2020**, *10*, 5734–5749. [CrossRef]
8. Sharma, N.; Das, T.; Kumar, S.; Bhosale, R.; Kabir, M.; Ogale, S.B. Photocatalytic Activation and Reduction of CO_2 to CH_4 over Single Phase Nano Cu_3SnS_4: A Combined Experimental and Theoretical Study. *ACS Appl. Energy Mater.* **2019**, *2*, 5677–5685. [CrossRef]
9. Li, C.; Xu, Y.; Tu, W.; Chen, G.; Xu, R. Metal-free photocatalysts for various applications in energy conversion and environmental purification. *Green Chem.* **2017**, *19*, 882–899. [CrossRef]
10. Rahman, M.Z.; Kibria, G.; Mullins, C.B. Metal-free photocatalysts for hydrogen evolution. *Chem. Soc. Rev.* **2020**, *49*, 1887–1931. [CrossRef]
11. Serpone, N.; Emeline, A.V. Semiconductor photocatalysis—Past, present, and future outlook. *J. Phys. Chem. Lett.* **2012**, *3*, 673–677. [CrossRef]
12. Rajendran, S.; Gracia, F.; Stephen, A. *Basic Principles, Mechanism, and Challenges of Photocatalysis*; Springer: Berlin/Heidelberg, Germany, 2017.
13. Nakata, K.; Fujishima, A. TiO_2 photocatalysis: Design and applications. *J. Photochem. Photobiol. C Photochem. Rev.* **2012**, *13*, 169–189. [CrossRef]
14. Lee, K.; Yoon, H.; Ahn, C.; Park, J.; Jeon, S. Strategies to improve the photocatalytic activity of TiO_2: 3D nanostructuring and heterostructuring with graphitic carbon nanomaterials. *Nanoscale* **2019**, *11*, 7025–7040. [CrossRef] [PubMed]
15. Dong, H.; Zeng, G.; Tang, L.; Fan, C.; Zhang, C.; He, X.; He, Y. An overview on limitations of TiO_2-based particles for photocatalytic degradation of organic pollutants and the corresponding countermeasures. *Water Res.* **2015**, *79*, 128–146. [CrossRef]

16. Kanakaraju, D.; Wong, S.P. Photocatalytic Efficiency of TiO_2-Biomass Loaded Mixture for Wastewater Treatment. *J. Chem.* **2018**, *2018*, 4314969. [CrossRef]
17. Wang, H.; Zhang, L.; Chen, Z.; Hu, J.; Li, S.; Wang, Z.; Liu, J.; Wang, X. Semiconductor heterojunction photocatalysts: Design, construction, and photocatalytic performances. *Chem. Soc. Rev.* **2014**, *43*, 5234–5244. [CrossRef] [PubMed]
18. Ariyanti, D.; Mukhtar, S.; Ahmed, N.; Liu, Z.; Dong, J.; Gao, W. Surface modification of TiO_2 for visible light photocatalysis: Experimental and theoretical calculations of its electronic and optical properties. *Int. J. Mod. Phys. B* **2020**, *34*, 1–8. [CrossRef]
19. Huang, F.; Yan, A.; Zhao, H. Influences of Doping on Photocatalytic Properties of TiO_2 Photocatalyst. *Semicond. Photocatal. Mater. Mech. Appl.* **2016**. [CrossRef]
20. Shifu, C.; Lei, C.; Shen, G.; Gengyu, C. The preparation of coupled WO_3/TiO_2 photocatalyst by ball milling. *Powder Technol.* **2005**, *160*, 198–202. [CrossRef]
21. Cano-Casanova, L.; Amorós-Pérez, A.; Lillo-Ródenas, M.A.; Román-Martínez, M. Effect of the preparation method (sol-gel or hydrothermal) and conditions on the TiO_2 properties and activity for propene oxidation. *Materials* **2018**, *11*, 2227. [CrossRef]
22. Sun, Q.; Hu, X.; Zheng, S.; Sun, Z.; Liu, S.; Li, H. Influence of calcination temperature on the structural, adsorption and photocatalytic properties of TiO_2 nanoparticles supported on natural zeolite. *Powder Technol.* **2015**, *274*, 88–97. [CrossRef]
23. Yamazaki, S.; Takaki, D.; Nishiyama, N.; Yamazaki, Y. Factors affecting photocatalytic activity of TiO_2. *Curr. Dev. Photocatal. Photocatal. Mater.* **2020**, 23–38. [CrossRef]
24. Kumar, A. A Review on the Factors Affecting the Photocatalytic Degradation of Hazardous Materials. *Mater. Sci. Eng. Int. J.* **2017**, *1*, 1–10. [CrossRef]
25. Li, D.; Song, H.; Meng, X.; Shen, T.; Sun, J.; Han, W.; Wang, X. Effects of particle size on the structure and photocatalytic performance by alkali-treated TiO_2. *Nanomaterials* **2020**, *10*, 546. [CrossRef] [PubMed]
26. Chen, Y.-F.; Lee, C.-Y.; Yeng, M.-Y.; Chiu, H.-T. The effect of calcination temperature on the crystallinity of TiO_2 nanopowders. *J. Cryst. Growth* **2003**, *247*, 363–370. [CrossRef]
27. Phromma, S.; Wutikhun, T.; Kasamechonchung, P.; Eksangsri, T.; Sapcharoenkun, C. Effect of calcination temperature on photocatalytic activity of synthesized TiO_2 nanoparticles via wet ball milling sol-gel method. *Appl. Sci.* **2020**, *10*, 993. [CrossRef]
28. Catauro, M.; Tranquillo, E.; Poggetto, G.D.; Pasquali, M.; Dell'Era, A.; Vecchio, S. Influence of the heat treatment on the particles size and on the crystalline phase of TiO_2 synthesized by the sol-gel method. *Materials* **2018**, *11*, 2364. [CrossRef]
29. Yudoyono, G.; Ichzan, N.; Zharvan, V.; Daniyati, R.; Santoso, H.; Indarto, B.; Pramono, Y.H.; Zainuri, M.; Darminto, D. Effect of calcination temperature on the photocatalytic activity of TiO_2 powders prepared by co-precipitation of $TiCl_3$. *AIP Conf. Proc.* **2016**, *1725*, 020099. [CrossRef]
30. Luttrell, T.; Halpegamage, S.; Tao, J.; Kramer, A.; Sutter, E.A.; Batzill, M. Why is anatase a better photocatalyst than rutile?—Model studies on epitaxial TiO_2 films. *Sci. Rep.* **2015**, *4*, 4043. [CrossRef]
31. Hurum, D.; Agrios, A.; Crist, S.; Gray, K.; Rajh, T.; Thurnauer, M. Probing reaction mechanisms in mixed phase TiO_2 by EPR. *J. Electron Spectrosc. Relat. Phenom.* **2006**, *150*, 155–163. [CrossRef]
32. Wei, Y.; Tokina, M.V.; Benderskii, A.V.; Zhou, Z.; Long, R.; Prezhdo, O.V. Quantum dynamics origin of high photocatalytic activity of mixed-phase anatase/rutile TiO_2. *J. Chem. Phys.* **2020**, *153*, 044706. [CrossRef] [PubMed]
33. Paul, S.; Choudhury, A. Investigation of the optical property and photocatalytic activity of mixed phase nanocrystalline titania. *Appl. Nanosci.* **2014**, *4*, 839–847. [CrossRef]
34. Bak, T.; Li, W.; Nowotny, J.; Atanacio, A.J.; Davis, J. Photocatalytic Properties of TiO_2: Evidence of the Key Role of Surface Active Sites in Water Oxidation. *J. Phys. Chem. A* **2015**, *119*, 9465–9473. [CrossRef] [PubMed]
35. Chong, M.N.; Vimonses, V.; Lei, S.; Jin, B.; Chow, C.W.; Saint, C.P. Synthesis and characterisation of novel titania impregnated kaolinite nano-photocatalyst. *Microporous Mesoporous Mater.* **2009**, *117*, 233–242. [CrossRef]
36. Shtyka, O.; Ciesielski, R.; Kedziora, A.; Maniukiewicz, W.; Dubkov, S.; Gromov, D.; Maniecki, T.P. Photocatalytic Reduction of CO_2 Over Me (Pt, Pd, Ni, Cu)/TiO_2 Catalysts. *Top. Catal.* **2020**, *63*, 113–120. [CrossRef]
37. Valencia, S.; Marín, J.M.; Restrepo, G. Study of the bandgap of synthesized titanium dioxide nanoparticules using the sol-gel method and a hydrothermal treatment. *Open Mater. Sci. J.* **2010**, *4*, 9–14. [CrossRef]
38. Dette, C.; Pérez-Osorio, M.A.; Kley, C.S.; Punke, P.; Patrick, C.E.; Jacobson, P.; Giustino, F.; Jung, S.J.; Kern, K. TiO_2 anatase with a bandgap in the visible region. *Nano Lett.* **2014**, *14*, 6533–6538. [CrossRef]
39. Lin, H.; Huang, C.; Li, W.; Ni, C.; Shah, S.I.; Tseng, Y.-H. Size dependency of nanocrystalline TiO_2 on its optical property and photocatalytic reactivity exemplified by 2-chlorophenol. *Appl. Catal. B Environ.* **2006**, *68*, 1–11. [CrossRef]
40. Vajda, K.; Saszet, K.; Kedves, E.; Kása, Z.; Danciu, V.; Baia, L.; Magyari, K.; Hernádi, K.; Kovács, G.; Pap, Z.; et al. Shape-controlled agglomeration of TiO_2 nanoparticles. New insights on polycrystallinity vs. single crystals in photocatalysis. *Ceram. Int.* **2016**, *42*, 3077–3087. [CrossRef]
41. Schaub, R.; Thostrup, P.; Lopez, N.; Lægsgaard, E.; Stensgaard, I.; Nørskov, J.K.; Besenbacher, F. Oxygen vacancies as active sites for water dissociation on rutile TiO_2(110). *Phys. Rev. Lett.* **2001**, *87*, 266104. [CrossRef]
42. Zhao, H.; Pan, F.; Li, Y. A review on the effects of TiO_2 surface point defects on CO_2 photoreduction with H_2O. *J. Materiomics* **2017**, *3*, 17–32. [CrossRef]
43. Ryu, Y.; Kim, K. Fabrication of antireflective hierarchical TiO_2 nanostructures by moth-eye patterning of anodic anodized nanotubes. *Opt. Express* **2018**, *26*, 31490–31499. [CrossRef] [PubMed]

44. Kuo, Y.-H.; Chen, H.-T.; Yen, F.-L.; Lu, W.-C.; Kuo, C.-W.; Wang, M.-C. Preparation of TiO_2 Nanocrystallite Powders Coated with 9 mol % ZnO for Cosmetic Applications in Sunscreens. *Int. J. Mol. Sci.* **2012**, *13*, 1658–1669. [CrossRef] [PubMed]
45. Zhang, J.; Zhou, P.; Liu, J.; Yu, J. New understanding of the difference of photocatalytic activity among anatase, rutile and brookite TiO_2. *Phys. Chem. Chem. Phys.* **2014**, *16*, 20382–20386. [CrossRef]
46. Wu, C.Y.; Tu, K.J.; Deng, J.P.; Lo, Y.S.; Wu, C.H. Markedly enhanced surface hydroxyl groups of TiO_2 nanoparticles with Superior water-dispersibility for photocatalysis. *Materials* **2017**, *10*, 566. [CrossRef]
47. Bertóti, I.; Mohai, M.; Sullivan, J.; Saied, S. Surface characterisation of plasma-nitrided titanium: An XPS study. *Appl. Surf. Sci.* **1995**, *84*, 357–371. [CrossRef]
48. Stadnichenko, A.I.; Muravev, V.; Koscheev, S.V.; Zaikovskii, V.I.; Aleksandrov, H.A.; Neyman, K.M.; Boronin, A.I. Study of active surface centers of Pt/CeO2 catalysts prepared using radio-frequency plasma sputtering technique. *Surf. Sci.* **2019**, *679*, 273–283. [CrossRef]
49. Stadnichenko, A.I.; Svintsitskiy, D.; Kibis, L.S.; Fedorova, E.A.; Stonkus, O.; Slavinskaya, E.; Lapin, I.N.; Fakhrutdinova, E.; Svetlichnyi, V.A.; Romanenko, A.; et al. Influence of titania synthesized by pulsed laser ablation on the state of platinum during ammonia oxidation. *Appl. Sci.* **2020**, *10*, 4699. [CrossRef]